Available online at www.sciencedirect.com
ScienceDirect
Journal of Power Sources 172 (2007) 100–107
JOURNAL OF POWER SOURCES
www.elsevier.com/locate/jpowsour

Small stack performance of intermediate temperature-operating solid oxide fuel cells using stainless steel interconnects and anode-supported single cell

Joongmyeon Bae [a,*], Sungkwang Lim [a], Hyunjin Jee [b], Jung Hyun Kim [a], Young-Sung Yoo [c], Taehee Lee [c]

[a] *Korea Advanced Institute of Science and Technology (KAIST), Daejeon 305-701, Republic of Korea*
[b] *Agency for Defense Development (ADD), Jochiwongil 462, Yuseong, Daejeon, Republic of Korea*
[c] *Korea Electric Power Research Institute (KEPRI), Daejeon 305-380, Republic of Korea*

Received 30 October 2006; received in revised form 24 January 2007; accepted 24 January 2007
Available online 16 February 2007

Abstract

We are developing 1 kW class solid oxide fuel cell (SOFC) system for residential power generation (RPG) application supported by Korean Government. Anode-supported single cells with thin electrolyte layer of YSZ (yttria-stabilized zirconia) or ScSZ (scandia-stabilized zirconia) for intermediate temperature operation (650–750 °C), respectively, were fabricated and small stacks were built and evaluated. The LSCF/ScSZ/Ni-YSZ single cell showed performance of 543 mW cm^{-2} at 650 °C and 1680 mW cm^{-2} at 750 °C.

The voltage of 15-cell stack based on 5 cm × 5 cm single cell (LSM/YSZ/Ni-YSZ) at 150 mW was 12.5 V in hydrogen as fuel of 120 sccm per cell at 750 °C and decreased to about 10.9 V at 500 h operation time. A 5-cell stack based on the LSCF/YSZ/FL/Ni-YSZ showed the maximum power density of 30 W, 25 W and 20 W at 750 °C, 700 °C and 650 °C, respectively. LSCF/ScSZ/Ni-YSZ-based stack showed better performance than LSCF/YSZ/Ni-YSZ stack from the experiment temperature range. *I–V* characteristics by using hydrogen gas and reformate gas of methane as fuel were investigated at 750 °C in LSCF/ScSZ/FL/Ni-YSZ-based 5-cell stack.

Keywords: Solid oxide fuel cell (SOFC); Residential power generation (RPG); Balance-of-plant (BOP); Yttria-stabilized zirconia (YSZ); Scandia-stabilized zirconia (ScSZ)

1. Introduction

Fuel cell is an electrochemical device which converts chemical energy from the reaction of a fuel (H_2, CH_4, natural gas) with an oxidant (O_2, air) directly into electrical energy. Fuel cell has high efficiency, low environmental impact and modularity. The advantage of fuel cell can be used for various application such as mobile power, automotives, residential power generation system [1]. SOFC is comprised of ceramic materials and operated at high temperatures ranges of 650–1000 °C. It has many advantages over conventional power-generating systems in terms of efficiency, reliability, modularity, fuel flexibility, and environmental friendliness. Especially, SOFC offers the possibility of combined generation of electricity and heat, thereby can be very efficient.

Lower operating temperature of SOFC (650–750 °C) gives many opportunities to select materials for interconnects and balance-of-plant (BOP) widely. To reach desirable power density at 650–750 °C as exploited at 900 °C, Planar anode-supported thin YSZ electrolyte (∼10 μm) structure was adopted. In planar geometry, an anode-supported structure presents advantages over a cathode-supported cell such as cell performance and mechanical strength [2,3].

In this paper, we investigated performances of single cells of YSZ and ScSZ as electrolytes extensively. The 15-cell and 60-cell stacks by using Inconel as interconnects were fabricated and the performance were analyzed, various 5-cell stacks comprised of 5 cm × 5 cm, and 10 cm × 10 cm cell were built and operated by using ferritic stainless steels as interconnects for intermediate temperature operations (650–750 °C). *I–V*

* Corresponding author. Tel.: +82 42 869 3045; fax: +82 42 869 8207
E-mail address: jmbae@kaist.ac.kr (J. Bae).

0378-7753/$ – see front matter © 2007 Elsevier B.V. All rights reserved.
doi:10.1016/j.jpowsour.2007.01.093

characteristics of 5-cell stacks were investigated by using not only hydrogen but also reformate gases as fuels.

2. Experiments

2.1. Single cell fabrication

Nickel oxide (NiO) and yttria-stabilized zirconia powders ($ZrO_2 + 8Y_2O_3$, 8YSZ) were primarily mixed and milled together at 50 wt%:50 wt% of powder mixtures to fabricate anode-supported type SOFC. Twenty-four volume percent graphite powders as pore-former and organic binder were mixed in the NiO–8YSZ mixtures with ethyl alcohol, and the mixtures were dried in an oven. The NiO–8YSZ powder mixture were isostatically pressed using a rectangular mold and heat-treated at 1400 °C for an hour to prepare a pre-sintered anode substrate. The size of anode substrate was about 6 cm × 6 cm with a thickness of 2 mm. Subsequently, the YSZ or ScSZ (10 mol% Sc_2O_3 + 1 mol% $CeO_2 + ZrO_2$, 10ScSZ) was coated on the substrate by slurry coating technique and the coated samples were sintered at 1550 °C for 2 h to form a dense electrolyte layer with a thickness of about 20 μm. The final size of sintered cell size was reduced to 5 cm × 5 cm and the thickness of 1.8 mm.

Citrate method was used to synthesize LSM ($La_{0.8}Sr_{0.2}MnO_3$) or LSCF ($La_{0.6}Sr_{0.4}Co_{0.2}Fe_{0.8}O_{3-\delta}$) as cathode materials [4]. The LSM and LSCF powders were calcinated at 800 °C for 1 h and at 1000 °C for 8 h, respectively after coating on the anode-supported cells. X-ray diffraction patterns were analyzed to confirm single perovskite phases of LSM and LSCF. The cathode materials were printed with thickness of 30 μm and heat-treated at 1100 °C for 2 h. The final products of anode-supported single cells have an activate cathode area of 4.7 cm × 4.7 cm. When the anode-supported cells were fabricated as the size of 10 cm × 10 cm, the active area of cathode were 9.7 cm × 9.7 cm. The protective layer of CeO_2–Gd_2O_3 was deposited between LSCF and YSZ (or ScSZ) to inhibit undesired chemical reaction between two layers.

2.2. Stack preparation

2.2.1. Stack using Inconel as interconnects for high temperature operation

Fig. 1 shows planar type SOFC stack, which consist of 15 and 60 cells by using Inconel as interconnects. A 60-cell module was stacked by 2 × 2 array configuration using 5 cm × 5 cm unit cells. The planar stack is based on internal manifold and cross flow-type structure. Low temperature-melting borosilicate was used for sealing of stack. Nickel felts were located between cells and interconnects of anode side for current collection. Flexibility of the nickel felts may also relieve undesired mechanical stress, which can be produced during heating up the stack. Inconel mesh coated with LSM–silver paste was introduced for current collection of cathode side. Inconel interconnect surface was also coated with silver paste to prohibit oxidation. Measurement and monitoring of voltages at the stacks were carried out for each layer.

2.2.2. Stack using stainless steel as interconnects for intermediate temperature operation

Ferritic stainless steels were used as interconnects at 650–750 °C. The metallic interconnects have several advantaged as follows: (1) The coefficient of thermal expansion (CTE) of ferritic stainless steel alloys is close to that of other cell components. (2) Stainless steels such as 430 or 446 ferritic alloys, are relatively cheap. Several shorts stacks as seen in Figs. 8 and 9 were built by using ferritic stainless steel (STS 430) as interconnects for intermediate temperature operation. However, The oxidizing environment of cathode side raises problems of undesired high contact resistance due to oxidation on the surface of interconnects. Cr poisoning to cathode from volatile chromium species notably $CrO_2(OH)_2$ from the ferritic interconnects is recognized as another serious degradation problems of SOFC stack [5]. To overcome these problems, composite paste of LSM and silver was fabricated and coated at the side of cathode of STS 430 interconnect. At cathode side, Inconel mesh coated with silver paste were introduced and Ni felt were used at anode side for current collection. Voltage was separately measured and monitored by

Fig. 1. Photographs of (a) 15-cell and (b) 60-cell stack using Inconel as interconnects.

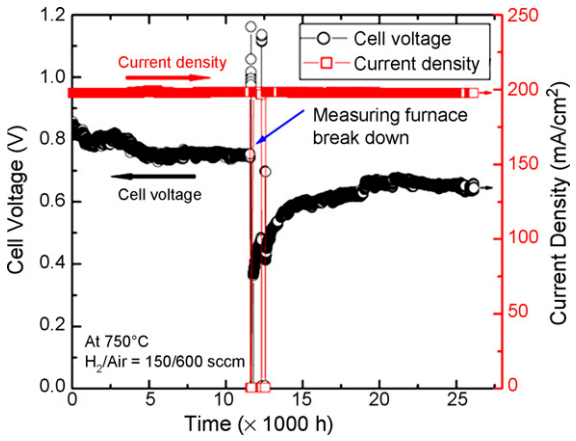

Fig. 2. Long-term performance of single cell over 3.5 years. Single cell consists of LSM, YSZ and Ni-YSZ. Two hundred milliamperes per centimeter square of current density is applied and the cell voltage is monitored.

multimeter for each layer and the cell impedance was measured by frequency resonance analyzer (Solartron 1287/1260).

2.3. Stack operation with reformate gas of methane

A 5-cell SOFC stack comprised of LSCF/YSZ/Ni-YSZ was operated with a methane autothermal reformer. The apparatus for the operation is composed of reformer system and the stack. The reformer was a packed-bed type reactor and was located inside a furnace for control of the reaction temperature. Fuel and air was fed to the reformer in controlled flow rate by MFCs and HPLC pump was used to supply water to the reformer. The reformate gas from the reactor was fed to the stack directly through the pipe line which was heated by electrical heater for prevention of water condensation. Reformate gas composition was analyzed by a gas chromatography (Agilent 6890) occasionally to analyze the reformate gas composition.

3. Results and discussions

3.1. Single cell measurement

3.1.1. LSM/YSZ/Ni-YSZ single cell

Long-term durability of our single cell ($La_{0.8}Sr_{0.2}MnO_3$/YSZ/Ni-YSZ) has been measured over 3.5 years as seen in Fig. 2. The cell voltage has been measured with H_2/air flow = 150/600 sccm at 750 °C and 200 mA cm^{-2} of current density. The initial cell voltage was 0.85 V and the voltage was decreased to 0.77 V after 3000 h and remained as 0.77 V. The abrupt voltage drop occurred at about 12,000 h of test period due to the furnace failure. The performance was slowly recovered after furnace repair mainly due to slow recovery of current collection. The average degradation rate of single cell comprised of $La_{0.8}Sr_{0.2}MnO_3$/YSZ/Ni-YSZ was about 0.5%/1000 h. This test shows excellent long-term durability of our cell and the expected life time of cells will be order of 10^5 h.

3.1.2. LSCF/YSZ/functional layer (FL)/Ni-YSZ single cell

One of the main electrical losses when SOFC is operated at intermediate temperature ranges comes from high cathodic resistance [6,7]. To overcome this problem, the LSCF ($La_{1-x}Sr_xCo_{1-y}Fe_yO_{3-\delta}$) was used as cathode materials because of its high cathode performance due to the mixed ionic and electronic conductivity (MIEC) as reported by us [8,9].

Anode property was enhanced by introducing thin and relatively dense Ni-YSZ cermet as a functional layer (FL) and subsequently thick and relatively porous anode layer was fabricated as seen in Fig. 3(a). The thickness of FL was about 15 μm and the size of pore was about 1 μm, while average pore size of supportive anode was about 5 μm. The performance of single cell in Fig. 3(a) is shown at Fig. 4. Maximum power density was greatly enhanced as 1.2 W cm^{-2} at 750 °C and 0.36 W cm^{-2} at 650 °C from improvements of cathode and anode. These results are better than those of SOFCs that used the same single cell structure of LSCF/YSZ/Ni-YSZ showing 350 mW cm^{-2} [10], 1 W cm^{-2} [11] and 1.1 W cm^{-2} [12] at 750 °C respectively, and also 370 mW cm^{-2} with $Ce_{0.8}Gd_{0.2}O_2$ as buffer layer [13].

3.1.3. LSCF/ScSZ/FL/Ni-YSZ single cell

There is strong interest in scandia-stabilized zirconia (ScSZ) as electrolyte because ScSZ is known to exhibit higher conductivity as compared to yttria-stabilized zirconia (YSZ). The conductivity enhancement in the ScSZ material is attributed to the similarity in ionic radii between the host ion Zr and dopant Sc. The activation energy for the transport of oxygen ions in the ScSZ is also reduced as compared to the value of YSZ [14,15].

To improve the cell performance further at intermediate temperature, ScSZ was adopted as electrolyte as seen in Fig. 3(b). Thin and relatively dense functional layer (FL) of anode was coated between ScSZ and supportive anode plate to improve the

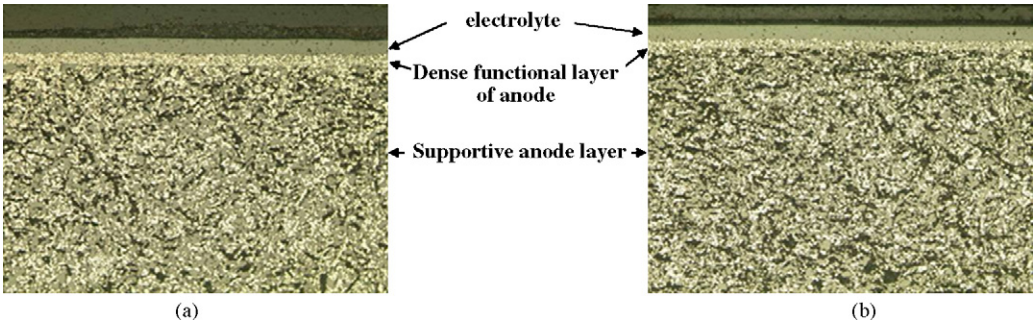

Fig. 3. Microstructures (cross-section view) of improved anode-supported single cell with (a) YSZ and (b) ScSZ electrolyte.

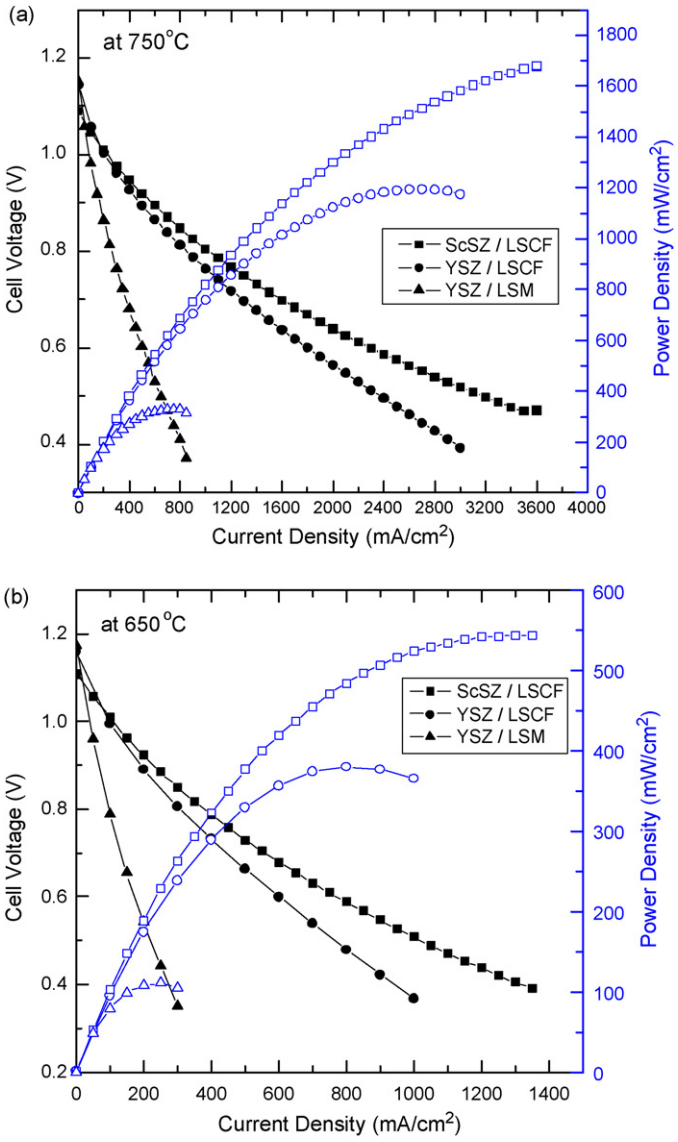

Fig. 4. Performance of LSM/YSZ/Ni-YSZ, LSCF/YSZ/FL (Ni-YSZ)/Ni-YSZ and LSCF/ScSZ/FL (Ni-YSZ)/YSZ cells using hydrogen as a fuel at (a) 750 °C and (b) 650 °C.

anode activity as shown in Fig. 3(b). By using ScSZ instead of YSZ as an electrolyte, we achieved another substantial enhancement for cell performance as shown in Fig. 4(a) and (b). At 750 °C, the ScSZ sample shows power density of 1.7 W cm^{-2} at 750 °C and 0.55 W cm^{-2} at 650 °C. LSCF/ScSZ/FL/Ni-YSZ single cell showed superior performance to those used the same electrolyte without FL, which exhibited 440 mW cm^{-2} [16] and 740 mW cm^{-2} [17] at 750 °C.

The single cell shows resistance of 0.34 Ω cm^2 at 750 °C and 0.75 Ω cm^2 at 650 °C from the analysis of ac impedance responses. The results of *I–V–P* curves according to the composition of cathode, electrolyte and existence of functional layer are summarized in Table 1. The cell of LSCF/ScSZ/FL (Ni-YSZ)/Ni-YSZ (anode) shows the best performance among the three types of structures; LSCF/ScSZ/FL (Ni-YSZ)/Ni-YSZ (anode), LSCF/YSZ/FL (Ni-YSZ)/Ni-YSZ (anode) and LSM/YSZ/Ni-YSZ (anode).

The cell of LSCF/ScSZ/FL (Ni-YSZ)/Ni-YSZ (anode) shows the five time higher power density than LSM/YSZ/Ni-YSZ (anode) at 650 °C and 750 °C. The performance enhancement is due to improved cathode, anode and electrolyte characteristics. LSCF has been reported as one of the best cathode materials due to its high MIEC. Functional layer of Ni-YSZ provides higher electrocatalytic area for better anode reaction and also better electronic path due to lower porosity.

The advantage of higher ionic conductivity of ScSZ compared to the values of YSZ was also clearly reflected in our single cell tests. IR (ohmic resistance) was reduced from 0.22 Ω cm^2 to 0.15 Ω cm^2 at 750 °C and from 0.5 Ω cm^2 to 0.34 Ω cm^2 at 650 °C by changing electrolyte from YSZ to ScSZ as shown in Fig. 5. Polarization losses from electrodes were also significantly reduced. ScSZ electrolyte cell showed 50% of performance increase due to lower ohmic and electrode polarization compared to YSZ system. The influence of electrolyte to electrode performance has to be investigated further in detail.

3.2. Stack operation

3.2.1. LSM/YSZ/Ni-YSZ-based 15-cell stack

A 15-cell stack was manufactured by using 5 cm × 5 cm cells of anode-supported LSM/YSZ/Ni-YSZ. The power output of the stack was about 60 W as shown in Fig. 6(a) when 150 sccm of H_2 at anode and 300 sccm of air at cathode per cell were supplied. When H_2 and Air supplies were increased to 300 sccm and 400 sccm, the power output was increased to the about 85 W due to decrease of concentration overpotentials [1]. The maximum power when H_2/air flow rates were 150/300 sccm was about 60 W at near 6 A. The maximum power was changed to 85 W at 9 A when H_2/air flow rates were changed to 300/450 sccm. The limiting current behavior due to concentration overpotentials are very clearly observed at the stack operation. The long-term stack performance was monitored as shown in Fig. 6(b). During 8000 h, Current density was loaded as 150 mA cm^{-2} for 8000 h continuously and the stack voltage was measured. At the first 300 h, the stack voltage was sharply decreased and then stabilized as 10 V. The initial degradation of the stack may be mainly due to oxidation of interconnects (Inconel 600) and increased contact resistance at cathode sides. In open circuit condition, 15 cells of the stack showed very uniform OCV (open circuit voltages). However, as current of the stack became increased, the stack exhibited significant unevenness as seen in Fig. 7. This problem was solved by changing stack and channel structures.

3.2.2. LSCF/YSZ/FL/Ni-YSZ-based 5-cell stack

A 5-cell stack was built using LSCF/YSZ/FL/Ni-YSZ single cells of 5 cm × 5 cm and STS 430 interconnects as shown in Fig. 8(a). The current–voltage–power characteristic curves (*I–V–P* curve) of the stack are presented in Fig. 8(b). The condition of reactant gases of H_2, N_2 (diluent gas of anode side) and air were 600 sccm, 400 sccm and 1500 sccm at 650 °C, 700 °C and 750 °C. The 5-cell stack showed the maximum power densities of 20 W, 25 W and 30 W at 650 °C, 700 °C and 750 °C, respectively.

Table 1
Summaries of maximum power density with various types of LSM/YSZ/Ni-YSZ, LSCF/YSZ/FL (Ni-YSZ)/Ni-YSZ and LSCF/ScSZ/FL (Ni-YSZ)/Ni-YSZ cells using hydrogen as a fuel at 750 °C and 650 °C

Temperature (°C)	Cell structure	Maximum power density (mW cm^{-2})	Current density (mA cm^{-2})
650	LSCF/ScSZ/FL (Ni-YSZ)/Ni-YSZ (anode)	543	1251
	LSCF/YSZ/FL (Ni-YSZ)/Ni-YSZ (anode)	380	799
	LSM/YSZ/Ni-YSZ (anode)	110	233
750	LSCF/ScSZ/FL (Ni-YSZ)/Ni-YSZ (anode)		3560
	LSCF/YSZ/FL (Ni-YSZ)/Ni-YSZ (anode)	1200	2610
	LSM/YSZ/Ni-YSZ (anode)	333	700

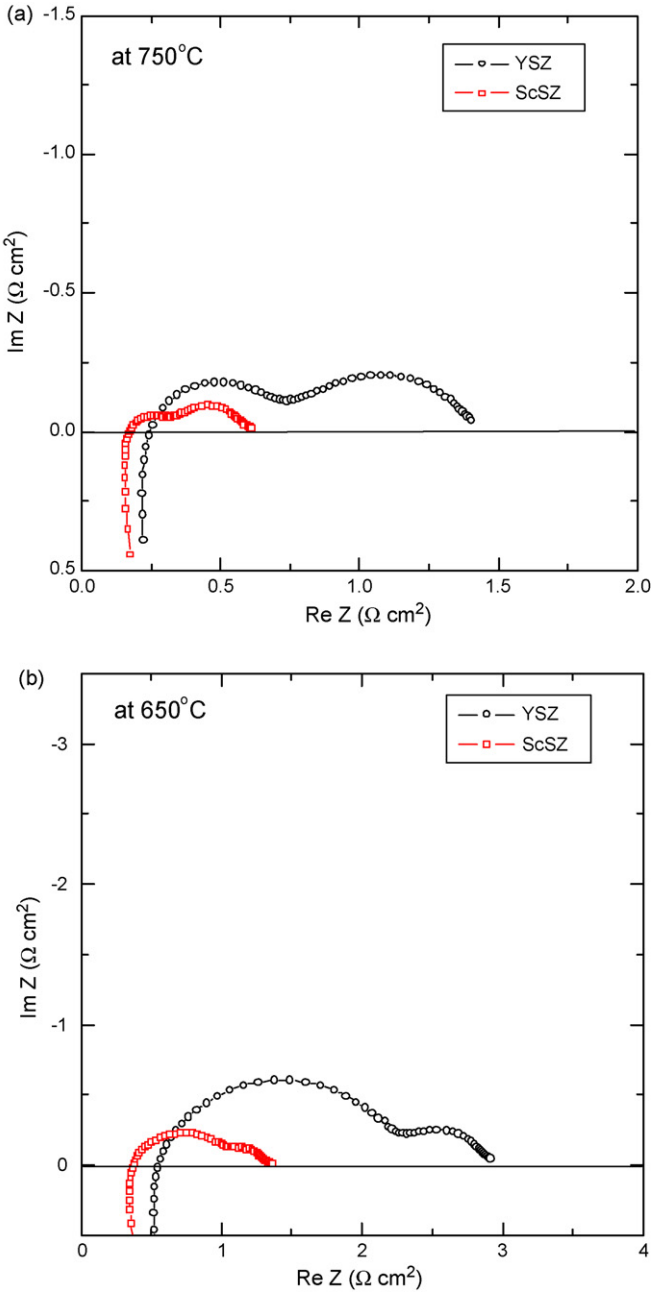

Fig. 5. ac impedance curves of the LSCF/ScSZ/Ni-YSZ and LSCF/YSZ/Ni-YSZ cells using hydrogen as a fuel at (a) 750 °C and (b) 650 °C.

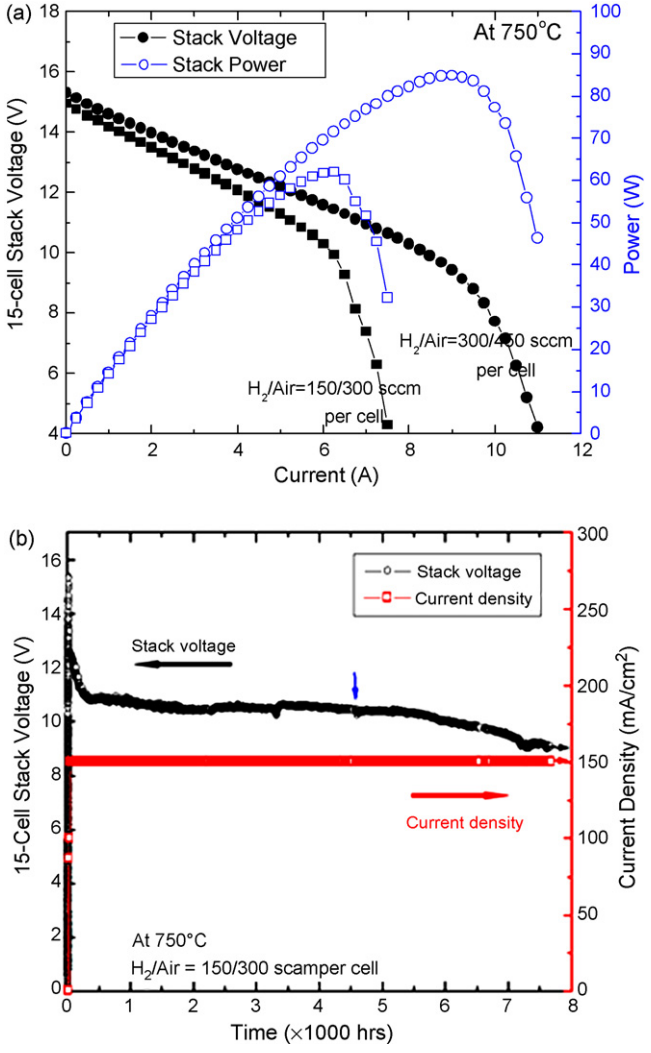

Fig. 6. Performance of 15-cell stack at 750 °C. (a) *I–V* Characteristics at 750 °C. (b) Long-term data for 15-cell stack at 750 °C.

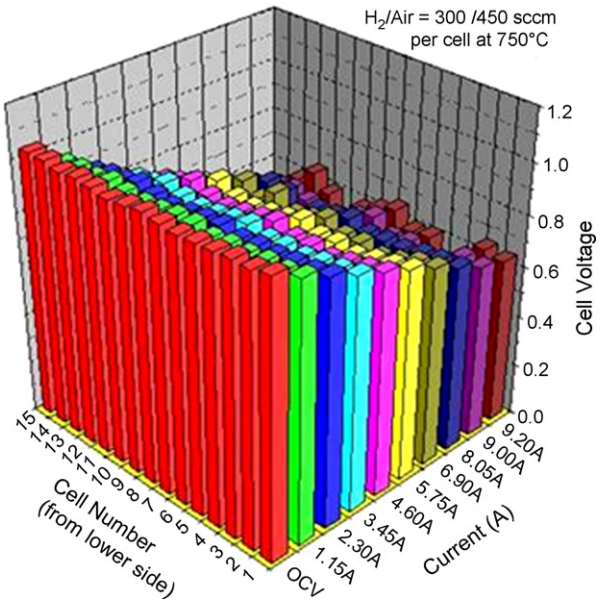

Fig. 7. Cell performance of 15-cell stack at 750 °C.

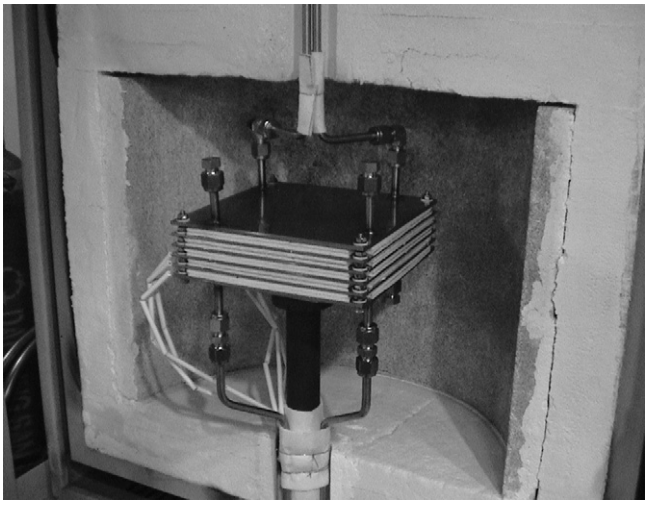

Fig. 9. Photograph of short stack (STS 430 was used as interconnects) of 10 cm × 10 cm, 5-cell stack.

When higher current was applied, the stack was unstable because one of the cells showed serious concentration polarization.

3.2.3. LSCF/ScSZ/FL/Ni-YSZ-based 5-cell stack

5-cell stacks were fabricated using STS 430 as interconnects and LSCF/ScSZ/FL/Ni-YSZ cells of 10 cm × 10 cm (Fig. 9). Long-term stack performance was monitored as shown in Fig. 10. Current densities were kept as constant and stack voltages were measured.

The stack using ScSZ showed sharp voltage degradation at the first 400 h operation as seen in Fig. 10, which was not shown in YSZ-based stack. Contact resistance problems due to oxidation of interconnects are gradually accumulated while the stack is continuously operated for several thousand hours as seen in Fig. 6(b). Therefore, the rapid degradation shown in Fig. 10 is not due to the oxidation of interconnects but the chemical instability of ScSZ.

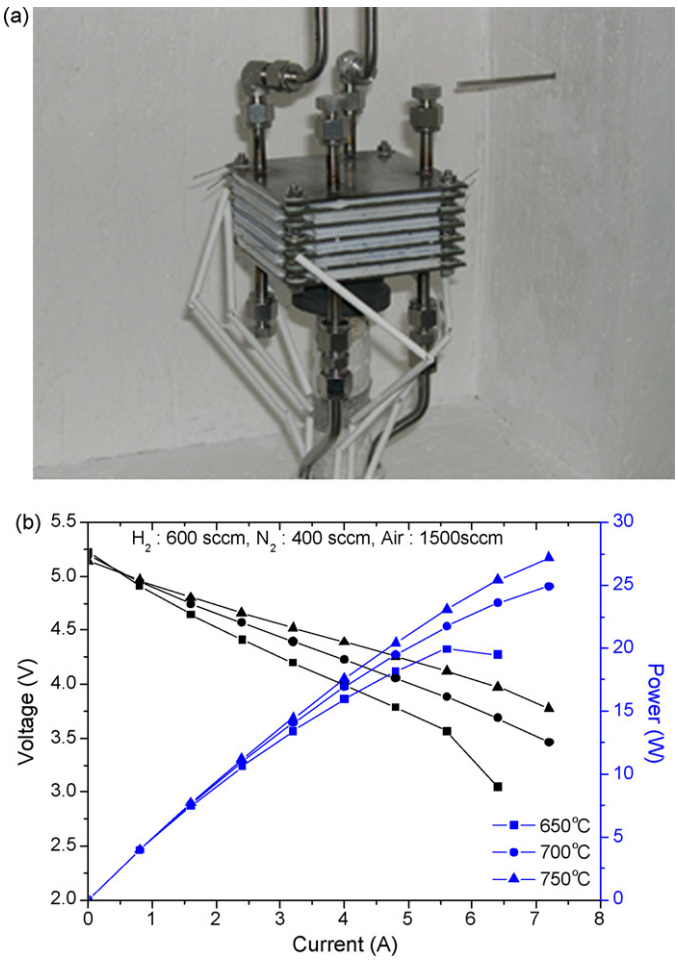

Fig. 8. Performance of 5-cell stack using LSCF/YSZ/Ni-YSZ cells and stainless steel. (a) 5 × 5 cm^2, 5-cell stack. (b) *I–V* curves of 5 cm × 5 cm, 5-cell stack at 650 °C, 700 °C and 750 °C.

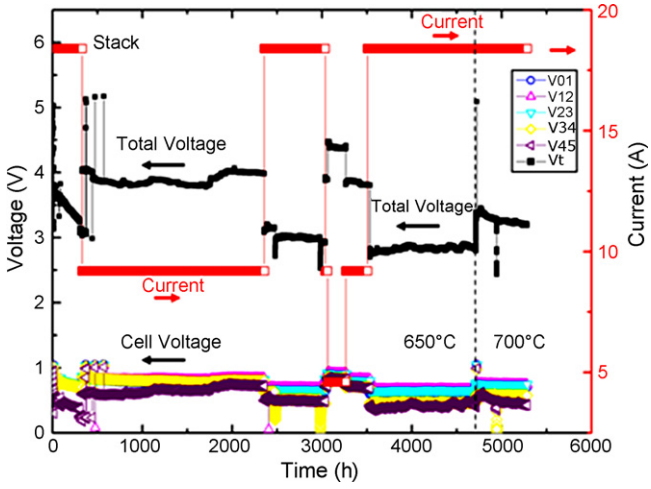

Fig. 10. Performance of (LSCF/ScSZ/FL/Ni-YSZ), 5-cell stack (10 cm × 10 cm) and single cell at 650 °C (STS 430 was used as interconnects in 5-cell stack).

The chemical instability of ScSZ been discussed at several references [17–20]. The instability lowers ionic conductivity of ScSZ and results in performance degradation in cells during long-term tests. This problem is under investigation in more detail and the results will be reported soon.

After the initial degradation, the stack was in continuous operation for 4700 h at 650 °C without significant degradations. After continuous operation at 650 °C, the operation temperature of the stack was increased to 700 °C, which is considered as practical operating temperature in a real residential power generation (RPG) system considering efficiency and stack size. The stack can produce higher power output and efficiency at 700 °C than 650 °C, but it may cause faster degradation, especially at stack due to the faster oxidation in cathode side of interconnect and decreased conductivity caused by unstable ScSZ phase. The stack performance is still under operation at 700 °C and the results will be reported later. However, before about 4700 h, each cell and/or stack showed uniform behavior.

3.3. SOFC 5-cell stack operation with reformate gases of methane

A small stack of 5-cell as LSCF/YSZ/FL/Ni-YSZ was operated with a methane autothermal reformer as shown in Fig. 11 under various anode fuel gas conditions. First, we operated the stack with synthetic gases of various H_2/CO ratios and monitored the effects of them. Synthetic gases were balanced by nitrogen and the ratio of $(CO + H_2)/N_2$ is set to the same value as the ratio of $(H_2 + CO)$/others in reformate gases from the methane autothermal reformer at reforming temperature of 700 °C. Fig. 12 shows *I–V* characteristic of each fuel condition. For synthetic gases, there were very little differences among *I–V* characteristic curves for different H_2/CO ratio. It indicates

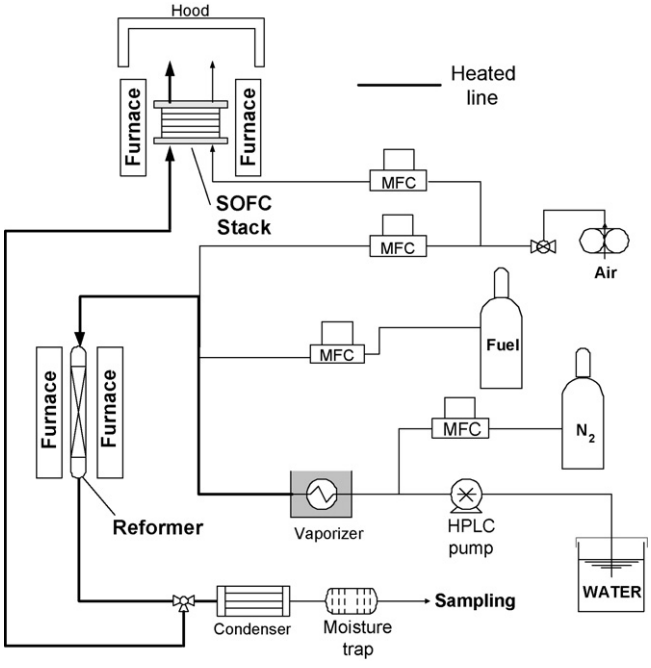

Fig. 11. Apparatus for SOFC stack operation with the methane reformer.

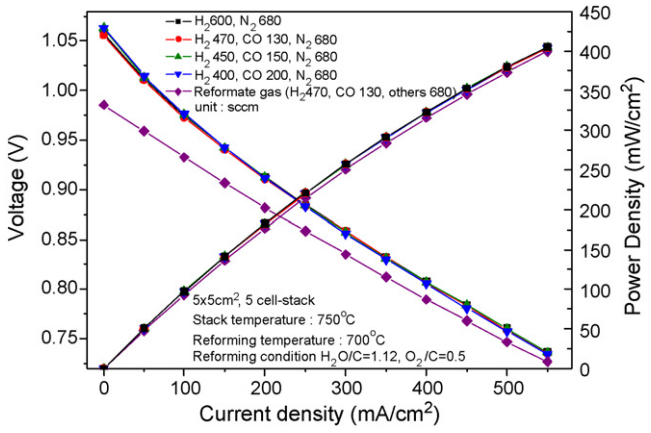

Fig. 12. Performance of LSCF/YSZ/FL/Ni-YSZ cells by using methane gas.

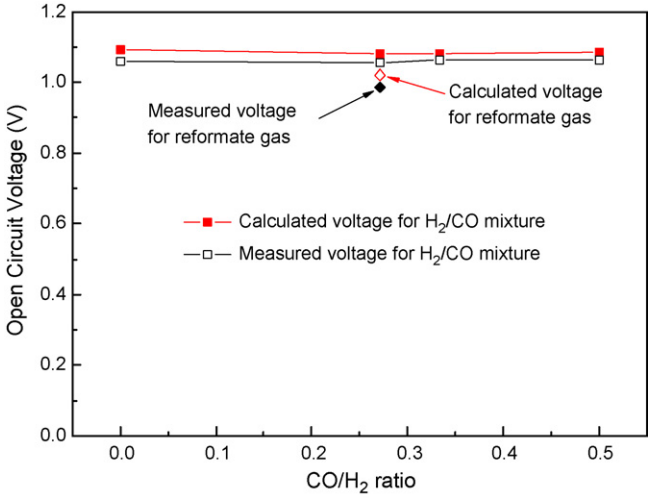

Fig. 13. Calculated and measured OCVs for H_2/CO mixtures and reformate gas.

that H_2/CO ratio dose not have strong effects on SOFC stack performance considering *I–V* characteristics. CO was nearly equivalent to H_2 as a fuel gas for SOFC cell under our experiment conditions. Therefore, H_2/CO ratio in the reformate gas would not be an important factor for SOFC when we operate a reformer for SOFC system. However, the *I–V* characteristic of the stack fed by reformate gas from autothermal reformer of methane is easily distinguished from those of the stack fed by synthetic gases. The difference was relatively large at the OCV condition. It is due to dilution effect of OCV of steam. OCV does not change for different H_2/CO rations, but shows significant difference when steam content increases as seen Fig. 13. Water content was about 10% in reformate gas while about 3% in synthetic gases feed which was humidified with bubbler.

4. Conclusions

4.1. Single cell experiment

Three types of anode-supported cell were developed to ensure high efficiency and performance for intermediate temperature operation. When thin and relatively dense functional layer (FL)

between electrolyte and anode to increase triple phase boundary (TPB) area and to decrease polarization was adopted. The performance of single cell was increased.

The performance of LSCF/YSZ/(functional-layered Ni-YSZ)/Ni-YSZ and LSCF/ScSZ/(functional-layered Ni-YSZ)/Ni-YSZ single cell showed maximum power density of 1.2 W cm^{-2} and 1.7 W cm^{-2} at 750 °C, respectively, and 0.36 W cm^{-2} and 0.55 W cm^{-2} at 650 °C. IR (ohmic resistance) was reduced from 0.22 Ω cm^2 to 0.15 Ω cm^2 at 750 °C and from 0.5 Ω cm^2 to 0.34 Ω cm^2 at 650 °C by changing electrolyte from YSZ to ScSZ.

4.2. Stack performance

Stack based on LSM/YSZ/Ni-YSZ was fabricated and its performance at temperature range 650–750 °C was measured. 15-Cell stack by using Inconel as interconnect material showed stable performance over 8000 h at 750 °C. The degradation of stack at initial state is considered to be caused mainly by undesired oxidation of interconnects. The ScSZ electrolyte cell showed 50% of performance increase due to lower ohmic and electrode polarization compared to YSZ system. However, ScSZ used stack showed rapid degradation at initial stage due to instability of ScSZ. Five-cell stack was operated by using syngas (H_2O/CO mixtures) and reformate gases of methane. H_2O/CO ratios in syngases does not have effects on SOFC stack performance. However, steam contents affect OCV due to dilute effect of Nernst potential. The stack showed comparable performance by using reformate gas to synthetic gases or hydrogen at operating conditions.

Acknowledgements

This work is outcome of the fostering project of the Best Lab and development of fundamental core-technology for low temperature-operating SOFC with high strength supported financially by the Ministry of Commerce, Industry and Energy (MOCIE) of Korea and supported by BK21 (Brain Korea 21) project from ministry of education & human resources development of Korea.

References

[1] J. Larminie, A. Dicks, Fuel Cell Systems Explained, 2nd ed., John Wiley & Sons, England, 2003, pp. 207–220.
[2] B.C.H. Steele, Solid State Ionics 1223 (1996) 86–88.
[3] S. de Souza, S.J. Visco, L.C. de Jonghe, Solid State Ionics 98 (1997) 57–61.
[4] Y.-S. Yoo, J.-H. Koh, J.-W. Park, H.C. Lim, Proceedings of the 7th International Symposium on Solid Oxide Fuel Cells, PV2001-16, Tsukuba, 2001, p. 590.
[5] J.W. Fergus, Mater. Sci. Eng. A 397 (1/2) (2005) 271–283.
[6] J.D. Kim, G.D. Kim, J.W. Moon, Y.I. Park, W.H. Lee, K. Kobayashi, M. Nagai, C.E. Kim, Solid State Ionics 143 (2001) 379–389.
[7] H.C. Yu, K.Z. Fung, J. Power Sources 133 (2004) 162–168.
[8] J.-M. Bae, B.C.H. Steele, Solid State Ionics 106 (1998) 247–253.
[9] B.C.H. Steele, J.-M. Bae, Solid State Ionics 106 (1998) 255–261.
[10] S.D. Kim, S.H. Hyun, J. Moon, J.-H. Kim, R.H. Song, J. Power Sources 139 (2005) 67–72.
[11] F. Tietz, V.A.C. Haanappel, A. Mai, J. Mertens, D. Stuver, J. Power Sources 156 (2006) 20–22.
[12] Z. Lei, Q. Zhua, L. Zhao, J. Power Sources 161 (2006) 1169–1175.
[13] W.-H. Kim, H.-S. Song, J. Moon, H.-W. Lee, Solid State Ionics 177 (2006) 3211–3216.
[14] O. Yamamoto, Y. Arati, Y. Takeda, N. Imanishi, Y. Mizutani, M. Kawai, Y. Nakamura, Solid State Ionics 79 (1995) (1995) 137–142.
[15] Y.-S. Yoo, H.-K. Seo, K.-S. Ahn, J.-M. Oh, J.-M. Bae, Proceedings of the 2nd International Conference on Fuel Cell Science Engineering and Technology, Rochester, NY, 2004, p. 39.
[16] K. Yamaji, H. Kishimoto, Y. Xiong, T. Horita, N. Sakai, H. Yokokawa, Solid State Ionics 175 (2004) 165–169.
[17] T.L. Nguyen, K. Kobayashi, T. Honda, Y. Iimura, K. Kato, A. Neghisi, K. Nozaki, F. Tappero, K. Sasaki, H. Shirahama, K. Ota, M. Dokiya, T. Kato, Solid State Ionics 174 (2004) 163–174.
[18] Y. Mizutani, M. Tamura, M. Kawai, O. Yamamoto, Solid State Ionics 72 (1994) 271–275.
[19] M. Hirano, E. Kato, J. Mater. Sci. 34 (1999) 1399–1405.
[20] Z. Lei, Q. Zhu, Solid State Ionics 176 (2005) 2791–2797.